Role of Electronic Excitation in the Amorphization of Ge-Sb-Te Alloys

Xian-Bin Li,[1] X. Q. Liu,[2] Xin Liu,[3,4] Dong Han,[1] Z. Zhang,[2,5] X. D. Han,[2,*] Hong-Bo Sun,[1] and S. B. Zhang[1,3,†]

[1]*State Key Laboratory on Integrated Optoelectronics, College of Electronic Science and Engineering, Jilin University, Changchun 130012, China*

[2]*Institute of Microstructure and Property of Advanced Materials, Beijing University of Technology, Beijing 100022, China*

[3]*Department of Physics, Applied Physics, & Astronomy, Rensselaer Polytechnic Institute, Troy, New York 12180, USA*

[4]*School of Chemistry, Dalian University of Technology, Dalian 116024, China*

[5]*State Key Laboratory of Silicon Materials and Department of Materials Science and Engineering, Zhejiang University, Hangzhou 310027, China*

(Received 13 September 2010; published 29 June 2011)

First-principles molecular dynamics simulation reveals the effects of electronic excitation in the amorphization of Ge-Sb-Te. The excitation makes the phase change an element-selective process, lowers the critical amorphization temperature considerably, for example, to below 700 K at a 9% excitation, and reduces the atomic diffusion coefficient with respect to that of melt by at least 1 order of magnitude. Noticeably, the resulting structure has fewer wrong bonds and significantly increased phase-change reversibility. Our results point to a new direction in manipulating ultrafast phase-change processes with improved controllability.

DOI: 10.1103/PhysRevLett.107.015501 PACS numbers: 61.43.Bn, 61.43.Dq, 64.60.Cn, 71.15.Pd

Phase-change materials such as chalcogenide Ge-Sb-Te alloys have been widely used in optical memory storage. Because of the extremely fast crystalline-amorphous transition, they are also expected to play a vital role in next-generation nonvolatile microelectronic memory devices [1–3]. Among the Ge-Sb-Te alloys, $Ge_2Sb_2Te_5$ (termed GST thereof) shows excellent performance both as optical and electrical memory devices. Although it is widely accepted that melting and subsequent quenching (as a result of thermal heating by laser or electric pulse) cause the rapid amorphization, the microscopic origin for the ultrafast phase change and for the exceptional reversibility is still unclear. Kolobov *et al.* proposed a model where Ge atoms in the rocksalt (RS) crystalline phase undergo umbrella flips from octahedral to tetrahedral sites [4]. Kim *et al.* [5], on the other hand, countered the proposal by suggesting that the amorphous structure is sustained essentially by *p*-like bonds as in the octahedral phase. First-principles molecular dynamics (MD) simulation can provide unique insights on the structural evolution [6]. For example, calculation by Hegedüs *et al.* [7] showed how connected square ring structures of the rocksalt phase, are formed during a melt cooling and how they are subsequently quenched into the amorphous phase.

However, a key element that has not received much attention is the role of the optical or electrical excitation in promoting the electrons from ground state to excited states. By taking electrons away from the bonding states and place them in the antibonding states, the excitation could potentially soften the lattice at temperatures well below its usual melting temperature [8]. In other words, the effect of either laser or electrical pulse on a solid may not simply be a ''heating effect,'' especially when the pulse is intense and the durations are as short as femtoseconds (which are significantly below the characteristic phonon time [9]). As early as 1979, Van Vechten proposed a theoretical adiabatic plasma model to explain pulsed laser annealing of silicon [10,11]. Experiments on plasma-induced phase transition in Si and GaAs [12,13] have lent support to Van Vechten's mechanism.

In this Letter, we show that electronic excitation plays an unexpected role in the amorphization of Ge-Sb-Te. First, the excitation is element selective, causing most Ge atoms to undergo coordination change from sixfold to four- and fivefold, but the effects on Sb and Te are noticeably smaller. Second, it lowers the critical amorphization temperature (T_a) considerably. For example, with a 9% electronic excitation, amorphization takes place at below 700 K and within only several picoseconds. Third, the amorphization process has 1 order of magnitude smaller diffusion coefficient with respect to that of melt. The resulting structure has more normal bonds and fewer wrong bonds, which explains the exceptional reversibility and durability of the material.

Our study employs the density functional theory with the generalized gradient approximation [14], as implemented in the VASP codes [15,16]. The electron-ion interaction is described by the Vanderbilt ultrasoft pseudopotential [17]. An energy cutoff of 140 eV is used for the plane wave expansion. To model RS GST, a supercell with 87 atoms (21 Ge, 18 Sb, 48 Te) and 9 cation vacancies is constructed. Atomic distributions are obtained according to the experimental suggestion given by Ref. [18]. Γ point is used in the Brillouin zone sampling. In the MD simulation, we used a 3-fs time step and the canonical *NVT* ensemble, in which the Nosé-Hoover thermostat is used to control the

temperature [19,20]. To calculate the melting point (T_m) for GST, we anneal a high-temperature melt at lower temperatures until the free energy starts to decrease accompanied by recrystallization. The calculated T_m is ~1000 K, in good agreement with experiment, ~900 K [21].

Using first-principles MD to study amorphization with optical excitation is currently a formidable task, as it requires the inclusion of electron-hole dynamics with time step in attoseconds. Here, we simplify the study by removing electrons from high-lying valence band states according to the strength of the excitation. In analogy to defect study, we used a jellium background to compensate for the loss of charge due to electron removal. Most of our studies assumed a 9% removal, corresponding to emptying all states in the energy window from 0.6 eV below the valence band maximum (VBM) to the VBM. We have estimated that a typical fs laser setup can readily generate excitations in excess of 9% [13,22] (see supplemental material [23]). To see if this excitation can effectively lower T_a, we carried out MD simulations at around or below T_m to as low as 600 K. Once the excitation is over, the excited electrons recombine with holes. To mimic this, we place the removed electron back. We then continue the MD simulation for some more time at 300 K to assess the effects of annealing.

Figure 1(a) shows for RS GST the element- and orbital-dependent density of states (DOS) near the VBM. As one might expect, the Te p states dominate the DOS in this energy range. Besides the Te, we also notice contributions from the Ge and Sb s orbitals, for which the Ge contribution is noticeably larger than that of Sb. Figures 1(b) and 1(c) show the real-space charge distribution at two different energy windows: from −0.66 to 0 eV and from −4.0 to −3.0 eV, respectively. We see that in Fig. 1(b) electrons reside primarily near Ge and its surrounding Te. In contrast, in Fig. 1(c) electrons reside primarily near Sb and its surrounding Te. In other words, the absorption of the excitation is cation selective.

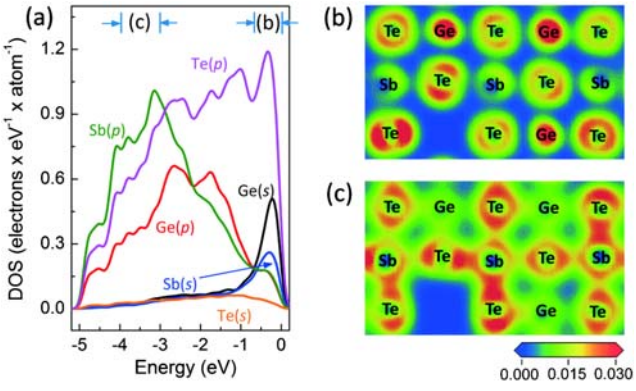

FIG. 1 (color online). (a) Orbital-decomposed local DOS normalized by the number of corresponding element, Ge, Sb, and Te, respectively. (b) and (c) Charge density plots in the (100) plane in unit of eÅ^{-3}: (b) is for states near the VBM from −0.66 to 0 eV and (c) is for states at deeper energies from −4 to −3 eV, as indicated by the letters (b) and (c) in panel (a).

Figure 2 shows a time evolution of the bond angles. To avoid a complication by the actual angle distribution (see, for example, the inset), we smooth the calculated angle distribution by a fitting and then plot in Fig. 2 the fitted peak positions for different elements. Figure 2(a) is for a 15 ps excitation at 700 K followed by a 9 ps quench at 300 K (Exc.Q). Figure 2(b) is for a liquid at 1100 K for 15 ps followed by a 9 ps quench at 300 K (Mel.Q). Note that the two curves have different starting points: RS GST for (a) and liquid GST for (b). The most striking difference between Exc.Q and Mel.Q in Fig. 2 is the response of Ge atoms. During the excitation, the Ge peak raises significantly to above 90° towards 100°. A crystal orbital Hamilton population analysis [24] (see Fig. S1 in the supplemental material [23]) reveals that the excitation removes electrons from the antibonding states mainly involving Ge-Te pairs for which the contribution from Ge s orbital is dominant [cf. Fig. 1(b)]. It has been pointed [25] out that a tetrahedral coordination is disfavored in RS GST because it has too many valence electrons. With the removal of the antibonding s electrons, however, the situation changes and the Ge will prefer the tetrahedral coordination with a 109.47° bond angle (for details, see Fig. S2 in the supplemental material [23]). This creates an instability that drives the amorphization of the GST under excitation at a significantly lower T_a than the T_m.

Figure 3 shows the snapshots for Exc.Q, along with the coordination number (CN). It starts at RS [3 (a)]. After

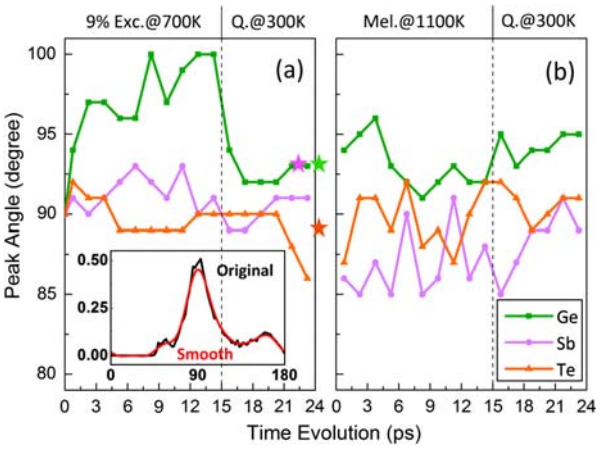

FIG. 2 (color online). Evolution of the peak angles during amorphization for (a) Exc.Q and (b) Mel.Q. Inset in (a) shows how to get the peak position by a smooth technique. The atomic densities are 0.0308 and 0.0297 atoms/Å^3, respectively. Both employ a hexagonal supercell [28] with $a = 17.47$ Å, $b = 17.41$ Å, $c = 10.68$ Å for Exc.Q and $a = 17.69$ Å, $b = 17.62$ Å, $c = 10.81$ Å for Mel.Q. Stars show the Exc.Q results at the end of the simulation with volume relaxation.

only 0.45 ps [3 (b)], the CN(Ge) is lowered from the original 6 to either 5 or 4 for every Ge, despite that visually the overall crystal structure remains largely intact. After 9 ps [3 (e)], the GST becomes amorphous. Importantly, such an amorphization takes place without any melting. This indicates that phase change under excitation is a solid-to-solid transition, which is expected to be considerably faster than amorphization via melting. Figure 3(f) shows that the amorphous structure remains after a 9 ps quench. The CNs are similar to those in Fig. 3(e) except for a significant population increase for CN(Sb) = 6. This is a consequence of placing back the removed electrons.

We also carried out the simulation at 600 K. In this case, amorphization also takes place during excitation, but the structure is back to RS after annealing. This suggests that for 9% excitation, T_a is between 600 and 700 K, which is substantially lower than the T_m. Note that T_a is the temperature for a direct amorphization within a few ps but T_m is not. In the absence of impurity in the MD simulation, the temperature for a comparable direct amorphization (without the excitation) is estimated to be at about 1600 K. In other words, the excitation effect is very significant.

So far the study is only concerned with holes in the valence band. In reality, the total effect due to excitation should be that of holes plus that of electrons. In Fig. S3 in the supplemental material [23], we show that the effect due to excited electrons in the conduction band is significantly smaller than that due to holes in the valence band. Hence, to a reasonable approximation the total effect can be replaced by holes in the valence band alone, as discussed here.

To measure the structural order, one usually use the pair correlation function (PCF). Figure 4(a) shows the average PCFs calculated at different time intervals during the simulation. If melting is an essential step in the phase-change process, one would expect the PCF for Exc.Q to approach that of liquid (Mel). However, throughout the excitation, the PCFs are not even close to that of Mel. One can easily see this in Fig. 4(b) where the peak at 2.9 Å is shown as a function of time. This difference suggests that the excitation-assisted amorphization is a solid-to-solid transition. Despite the lack of melting, however, the first three peaks, 2.89, 4.26, and 6.25 Å, in the final PCF (i.e., the 21–24 ps curve) agree with experiment, 2.77, 4.10, and 6.25 Å [26], respectively. This establishes that the final structure via the Exc.Q process is indeed amorphous and the phase transition has been completed. Figure 4(c) shows the mean square displacements (MSDs). One can fit the MSD by a linear curve to find the slope, which is proportional to the diffusion constant. The slope for excitation (Exc.) is about 15 times smaller than that for Mel. A significantly smaller MSD slope implies better reversibility.

Figures 5(a) and 5(b) show the change of the bond numbers (CBNs) with respect to the RS structure for Exc.Q and Mel.Q. We used 1.3 × (covalent radii) as the bond cutoffs to ensure that for the RS structure, CN(Ge/Sb) = 6. Next, we calculated the 1000 time-step average in the final states (between 21 and 24 ps). We then

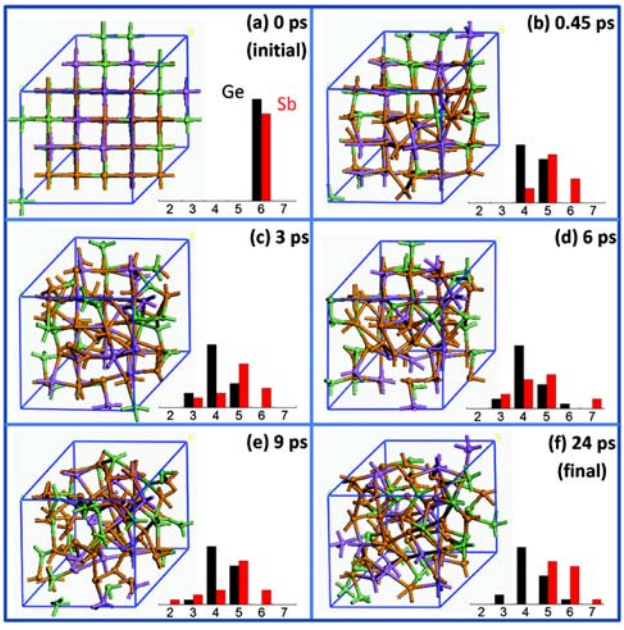

FIG. 3 (color online). Snapshots of a representative structural evolution with 9% excitation at 700 K. Green (light gray), purple (dark gray), and orange (medium gray) balls are Ge, Sb, and Te atoms, respectively. Histograms show the time evolution of the Ge and Sb coordination numbers (CNs).

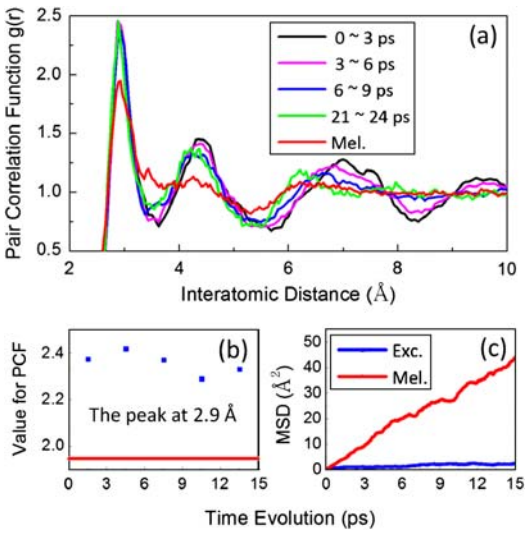

FIG. 4 (color online). (a) Time evolutions of the pair correlation function (PCF) during amorphization with 9% excitation at 700 K. (b) PCFs at 2.9 Å for Exc. (blue squares) and Mel. at 1100 K (red line). The PCF are averaged over 1000 frames. (c) The corresponding mean square displacements (MSDs).

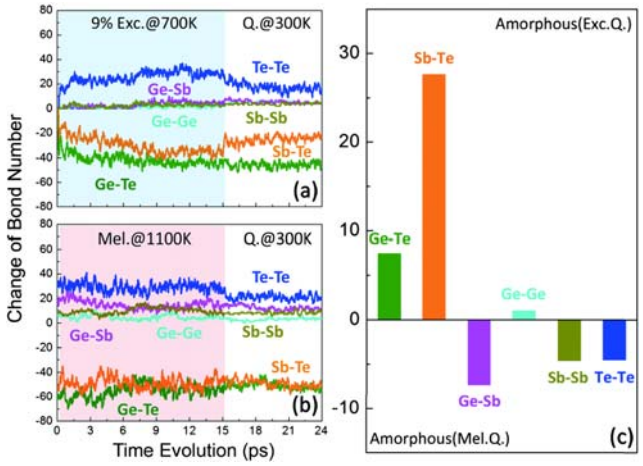

FIG. 5 (color online). (a) and (b) Change in the bond numbers (CBNs) for Exc.Q and Mel.Q with respect to the RS structure. (c) Difference in the CBNs between Exc.Q and Mel.Q final states.

calculated the difference between CBN(Exc.Q) and CBN (Mel.Q) and plotted the results in Fig. 5(c). It shows that, while tetrahedral Ge has comparable concentrations (Fig. S4, supplemental material [23]), Exc.Q has noticeably higher numbers of Ge-Te and Sb-Te bonds and generally less numbers of wrong bonds than Mel.Q. These are in agreement with the results in Figs. 3 and 4.

In conclusion, first-principles theory modeling and simulation reveal the significant impact of electronic excitation on the phase-change process in the GST which has not been addressed in the current prevailing theories. By this excitation, a solid-to-solid amorphization process can take place. Upon completion of the work, we learned that subnanosecond time-resolved x-ray absorption measurements provide experimental evidence that the amorphization process does not proceed via the molten state but is a photoassisted process [27]. These results offers new insights on how to better design and control the GST materials and processes to further increase the stability, reversibility, and speed for data storage.

This work was supported by National 973 program (Contract No. 2007CB935401), NSFC (Contract No. 60525412) and U.S. DOE/BES (Contract No. DE-SC0002623) and CMSN program. Professor W. Q. Tian, Professor H. Y. Wang, Dr. H. Wang, Dr. H. Li, and L. Wang are gratefully acknowledged for helpful discussions. We thank the High Performance Computing Center (HPCC) of Jilin University for calculation resource.

*xdhan@bjut.edu.cn
†zhangs9@rpi.edu

[1] S. R. Ovshinsky, Phys. Rev. Lett. **21**, 1450 (1968).
[2] N. Yamada *et al.*, J. Appl. Phys. **69**, 2849 (1991).
[3] M. Wuttig and N. Yamada, Nature Mater. **6**, 824 (2007).
[4] A. V. Kolobov *et al.*, Nature Mater. **3**, 703 (2004).
[5] J. J. Kim *et al.*, Phys. Rev. B **76**, 115124 (2007).
[6] F. Ercolessi, "A Molecular Dynamics Primer", available from http://www.fisica.uniud.it/~ercolessi/ (1997).
[7] J. Hegedüs and S. R. Elliott, Nature Mater. **7**, 399 (2008).
[8] M. Wautelet, Phys. Status Solidi B **138**, 447 (1986).
[9] S. K. Sundaram and E. Mazur, Nature Mater. **1**, 217 (2002).
[10] J. A. Van Vechten, R. Tsu, F. W. Saris, and D. Hoonhout, Phys. Lett. A **74**, 417 (1979).
[11] J. A. Van Vechten, R. Tsu, and F. W. Saris, Phys. Lett. A **74**, 422 (1979).
[12] E. N. Glezer, Y. Siegal, L. Huang, and E. Mazur, Phys. Rev. B **51**, 9589 (1995).
[13] K. Sokolowski-Tinten, J. Bialkowski, and D. von der Linde, Phys. Rev. B **51**, 14 186 (1995).
[14] J. P. Perdew and Y. Wang, Phys. Rev. B **45**, 13 244 (1992).
[15] G. Kresse and J. Furthmüller, Phys. Rev. B **54**, 11 169 (1996).
[16] G. Kresse and J. Furthmuller, Comput. Mater. Sci. **6**, 15 (1996).
[17] D. Vanderbilt, Phys. Rev. B **41**, 7892 (1990).
[18] T. Matsunaga, Y. Kubota, and N. Yamada, Acta Crystallogr. Sect. B **60**, 685 (2004).
[19] S. Nosé, Prog. Theor. Phys. Suppl. **103**, 1 (1991).
[20] D. M. Bylander and L. Kleinman, Phys. Rev. B **46**, 13 756 (1992).
[21] J. Kalb, F. Spaepen, and M. Wuttig, J. Appl. Phys. **93**, 2389 (2003).
[22] J. Siegel *et al.*, J. Appl. Phys. **103**, 023516 (2008).
[23] See supplemental material at http://link.aps.org/supplemental/10.1103/PhysRevLett.107.015501 for an estimate of the amount of excitation; COHP analysis; time-sequence of orbital-dependent DOS; effect due to excited electrons; and orbital-dependent DOS with and without excited holes.
[24] M. Wuttig *et al.*, Nature Mater. **6**, 122 (2007).
[25] M. Luo and M. Wuttig, Adv. Mater. **16**, 439 (2004).
[26] S. Kohara *et al.*, Appl. Phys. Lett. **89**, 201910 (2006).
[27] P. Fons *et al.*, Phys. Rev. B **82**, 041203(R) (2010).
[28] Z. M. Sun *et al.*, Phys. Rev. Lett. **102**, 075504 (2009).